

Disparate effects of an O₂ internal impurity on the elongation and quantum transport of gold and silver nanowires

S. Barzilai, F. Tavazza, and L. E. Levine

Citation: *J. Appl. Phys.* **114**, 074315 (2013); doi: 10.1063/1.4818956

View online: <http://dx.doi.org/10.1063/1.4818956>

View Table of Contents: <http://jap.aip.org/resource/1/JAPIAU/v114/i7>

Published by the [AIP Publishing LLC](#).

Additional information on *J. Appl. Phys.*

Journal Homepage: <http://jap.aip.org/>

Journal Information: http://jap.aip.org/about/about_the_journal

Top downloads: http://jap.aip.org/features/most_downloaded

Information for Authors: <http://jap.aip.org/authors>

ADVERTISEMENT



AIPAdvances

Now Indexed in
Thomson Reuters
Databases

Explore AIP's open access journal:

- Rapid publication
- Article-level metrics
- Post-publication rating and commenting

Disparate effects of an O₂ internal impurity on the elongation and quantum transport of gold and silver nanowires

S. Barzilai,^{a)} F. Tavazza, and L. E. Levine

MSED, Material Measurement Laboratory, National Institute of Standards and Technology,
 100 Bureau Drive, Stop 8553, Gaithersburg, Maryland 20899, USA

(Received 23 May 2013; accepted 5 August 2013; published online 21 August 2013)

In this work, we investigated the effects of an internal O₂ impurity on the conductance of elongated gold and silver nanowires (NWs) using density functional theory calculations. We found that the O₂ interacts with these metallic NWs very differently. In the case of gold NWs, the presence of an internal oxygen molecule locally strengthens the wire, therefore, forcing the phase transformations connected to the thinning process (3D to 2D and 2D to single atom chain) to occur far from the oxygen. As a consequence, towards the end of the elongation, the internal O₂ is located far from the main conductance channel and therefore has little influence on the conductance of the NW. In contrast, in silver NWs, the presence of an internal oxygen molecule involves a larger charge transfer from the metallic atoms to the oxygen, therefore, weakening the Ag-Ag binding. During the initial stages of the elongation, several metallic bonds adjacent to the impurity break, so that in most simulations the NW thinning takes place near the O₂. This thinning mechanism places the O₂ near the main conductance channel, therefore, significantly reducing the conductivity of the elongated silver NWs. For both metals, our findings agree well with the published experimental results. © 2013 AIP Publishing LLC. [<http://dx.doi.org/10.1063/1.4818956>]

I. INTRODUCTION

The demand for decreasing chip dimensions creates the need to scale down the size of both integrated circuits and interconnect wires. Gold and silver nanowires (NWs) can be thinned down to single atom chains (SACs) during tensile deformation. This ability makes them good candidates for applications such as nanoelectronics, as well as very attractive from a fundamental science point of view. This is exemplified by the many experimental^{1–15} and theoretical^{16–53} studies that have been carried out to characterize their electronic properties and to understand the influence of atomic configuration and impurities on their conductance.

The influence of molecular oxygen on the conductance of gold and silver NWs during elongation has been experimentally examined by Thijssen *et al.*^{14,15} Significant changes were found in the conductance histogram of Ag NWs at 4.2 K after exposure to O₂: a dominant conductance peak around 0.1 G₀ appeared, together with a large background below 1 G₀ (where G₀ = 2e²/h, with e as the electron charge and h as Planck's constant). In contrast, the conductance of Au NWs at the same temperature was hardly changed with the introduction of O₂ into the experimental chamber. In this case, the effect of the contaminant only started to be noticeable at higher temperatures: at 40 K, an additional conductance peak did appear at 0.1 G₀. Several theoretical attempts were made to understand the effect of oxygen on the conductance of Au or Ag^{48–53} NWs. It was found that when atomic oxygen is incorporated into a SAC of gold or silver, it increases the electron scattering and decreases the conductance. However, most of the studies considered atomic oxygen species which are already on a SAC. This consideration

neglects the effect of the O₂ original position prior to the elongation and its ability to dissociate and to reach the SAC zone. The only exceptions were the work of Jelínek *et al.*⁵⁰ and the work of Qi *et al.*⁵² Jelínek *et al.* neglect the dissociation stage but do show that atomic oxygen can reach the SAC during elongation of three-dimensional (3D) gold NWs. Qi *et al.* found that when the O₂ is on the silver SAC, it can incorporate into it during the elongation process, but did not address the ability of O₂ molecule to reach the SAC during elongation. Moreover, in an experimental system, a sample is created by “crashing” the tip of a metallic wire onto a flat metallic plate to form a contact junction. A nanowire is then formed by drawing the wire away from the plate. When a contaminant is *a priori* adsorbed on the tip or on the plate surface, it can be trapped in the contact junction and form an internal contaminant which can affect the measurements.

To study the effect of an internal O₂ molecule contamination on gold and silver NWs, and its ability to reach the SAC region during elongation, we simulated tensile deformation of 3D gold and silver NWs contaminated with an internal O₂ impurity. Different behavior was found for the two metals. In the case of gold NWs, the O₂ remained confined inside the NWs and never reached the SAC zone, while for the silver NWs, in most of the simulations, the O₂ was pushed from its internal site to the NW surface, and ended in or nearby the SAC. This difference results in dissimilar structural changes during the elongation of the two metals, and different conduction states for the NWs.

II. METHODOLOGY

Pure gold and silver NWs containing 115 atoms were built with (110) planes perpendicular to the NW axis

^{a)}On sabbatical leave from the Nuclear Research Center, Negev, Israel.

(Z axis), and contaminated NWs having the same size and orientation, were elongated along two directions (6° and 48° off the Z axis). At each tensile step, the grip atoms (two layers at each end of the wire) were translated by a fixed amount, while the remaining atoms were allowed to relax into a new configuration. For more detailed information, see Ref. 16. To simulate internal contamination in the NWs, one of the internal metallic atoms was replaced by an O_2 impurity. In this study, we considered two different sites: one in the center of the NW and one in the shoulder, adjacent to the rigid grip layers (Fig. 2). Prior to the elongation, for each site, three initial impurity orientations were selected for relaxation. In the case of Au NWs, we found that, at the end of the relaxation, all the initial orientations had converged to the same terminal orientation which was also identical for both the central and the shoulder sites: the O_2 had relaxed to the middle of its site, oriented $\approx 45^\circ$ with respect to the Z axis. In contrast, the O_2 inside the silver NWs relaxed to two possible configurations: (1) oriented $\approx 45^\circ$ with respect to the Z axis, as seen for the gold NWs, and (2) perpendicular to the Z axis. Orientation (1) has lower energy, and therefore, it was selected for most of the subsequent calculations. Orientation (2) was kept for additional calculations where the O_2 was placed in the center of the NWs. These relaxed structures were used as initial configurations for the NW elongation.

The calculations performed to elongate the nanowires were carried out in the framework of density functional theory (DFT) using the DMol³ code.^{54–56} This code employs localized basis sets, which make it fast and particularly well suited for cluster calculations. We used a real-space cutoff of 4 \AA and a double-zeta, atom-centered basis set (dnd). The exchange-correlation potential was treated within the Perdew-Burke-Ernzerhof (PBE) generalized gradient approximation (GGA) approach.⁵⁷ The ion core electrons of the Au and Ag were described by a hardness conserving semilocal pseudopotential (dspp),⁵⁸ and only the outer electrons were treated as valence electrons. To ensure that the results of the calculations are directly comparable, identical conditions were employed for all systems. The geometry optimization was performed using a conjugate gradient approach based on a delocalized internal coordinate scheme.^{59,60} The system was considered converged when the energy change was less than 10^{-4} eV ($6 \times 10^{-6} \text{ Ha}$) and the maximum atomic displacement was less than 10^{-4} \AA . The density of states (DOS) were computed using a Monkhorst-Pack scheme⁶¹ having $1 \times 1 \times 10$ k-point sampling and periodic boundary conditions. To avoid interactions between cells, a vacuum separation of 35 \AA was used in the x and y directions, while a continuation condition was utilized along the direction of the wire axis. It should be recalled that DFT calculations provide access to the DOS of the non-interacting Kohn-Sham reference system, rather than that of the fully interacting system of electrons,⁶² but the two systems may be expected to be qualitatively similar.

The conductance calculations were performed at zero bias using a non-equilibrium Green's function technique based on the Landauer formalism,⁶³ as implemented in the ATK package.^{22,64,65} The system was divided into three

regions: a left and a right electrode (made from Au for the gold NWs and Ag for the silver NWs), and a central scattering region between them. For the latter, we used the atomic configurations obtained by the DFT elongation. The attachment of the electrodes to the scattering zone was completely seamless since the grip atoms in the deformation simulations had been kept fixed into ideal FCC positions. Huckel tight binding⁶⁶ was utilized for all of the cluster-based configurations, using the Cerda parameterization⁶⁷ for Au and Ag, while the Hoffmann parameterization⁶⁸ was used for O and H atoms.

III. RESULTS

The effect of oxygen contamination on the conductance of gold and silver NWs during their elongation is shown in Fig. 1. The computational results are well correlated with the experimental results mentioned previously.^{14,15} At the late stages of elongation, the conductance of both pure NWs is around $\approx 1 G_0$, while the conductance of the contaminated NWs varies. In most of the gold NW simulations, the oxygen has only a small effect on the conductance; whereas for most of the silver NW simulations, the conductance decreases well below $1 G_0$. This difference is related to the location of the oxygen at this (late) stage of the elongation. Fig. 2 presents atomic configuration snapshots from tensile simulations of the impure gold and silver NWs. For the gold NW, during the entire elongation the impurity is surrounded by gold atoms and the phase transformations from 3D to 2D, and afterward to a SAC, occur far from the impurity location. This result was found in all of the gold + O_2 simulations, and explains the small effect the oxygen has on the computed conductance values (Fig. 1). The small decrease below $1 G_0$ is a well-known phenomenon and is related to the atomic configuration of the gold atoms.^{29,30,36} For the silver case, the oxygen interacts with the Ag atoms in a different manner; in most simulations, the O_2 was pushed out from its internal site to the surface of the NW. In only one simulation, where the oxygen was initially located in the shoulder, it did remain inside. These results demonstrate that, in the early stages of elongation, the Ag-Ag bonds in the vicinity of the oxygen are weakened, allowing the impurity to move towards the thinned out part of the wire (the main conductance channel) and therefore decreasing the conductance. At the latter stages of elongation, when the oxygen is already on the surface, the NW continues to thin down to a SAC. When this thinning occurs in the vicinity of the oxygen, the conductance decrease below $1 G_0$ but, when the thinning takes place away from the oxygen, a conductance level of $\approx 1 G_0$ was obtained.

Mulliken population analysis shows that 0.7 electrons are transferring from the silver atoms to the oxygen, while the gold atoms only transfer 0.1 electrons. Thus, even before causing structural changes in the NWs, the oxygen has a higher impact on the conductance of silver NWs than of gold ones. This can be seen in Fig. 1, observing the beginning of the elongation (where both NWs length are $\approx 15 \text{ \AA}$). At this stage, the conductance of both pure wires is $\approx 6.5 G_0$, but replacing one internal metallic atom with an O_2 molecule

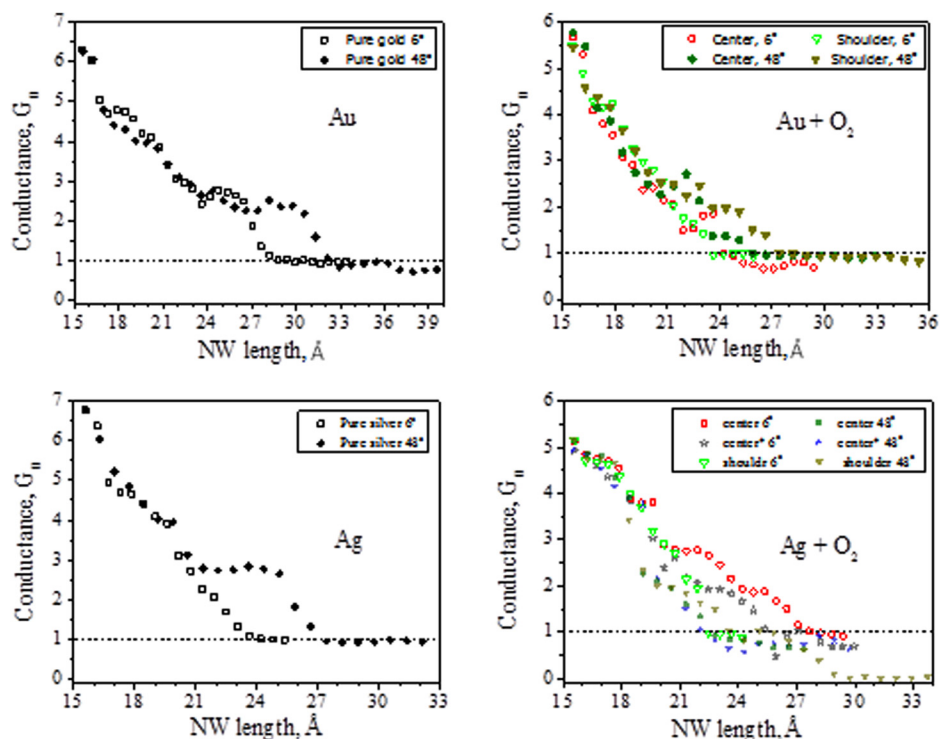


FIG. 1. The computed conductance of pure and contaminated NWs during elongation. The hollow and solid symbols represent a tensile direction of 6° and 48° off the Z axis, respectively. The triangular symbols refer to the NWs where the O_2 was placed in the shoulder, while the circles and the stars refer to the NWs that initially had O_2 in the center, oriented 45° and 90° from the Z axis, respectively.

decreases it to $\approx 5.5 G_0$ in the case of gold and to $\approx 5 G_0$ in the case of silver.

To further clarify the effect of the impurities on the conductance, the electronic properties and transmission pathways were computed for a variety of cases for pure and contaminated gold and silver NWs. Representative results are displayed in Fig. 3. Electron depletion was found for all of the gold and silver atoms in the vicinity of the O_2 impurity. For the gold NWs, during the entire elongation, the O_2 was surrounded by many gold atoms, and therefore, by several conductance channels. Each channel utilized only a fraction of the available electrons to feed the main transmission pathway, and therefore, the electron depletion hardly affected such a pathway (Fig. 3(a)). For the silver NWs, in

most of the cases, the O_2 moved away from its initial internal site toward the surface and then became incorporated in or near the bottleneck of the transmission pathway. In such a position, only one conductance channel exists so that the electron depletion around the O_2 (Fig. 3(b)) significantly decreases the availability of conducting electrons and increases the probability that such electrons are scattered. In the remaining cases, where the O_2 remained far from the main transmission pathway, the electron depletion hardly influenced the conductance, similar to what was found for the gold NWs.

To better understand the differences in the oxygen's behavior in the studied NWs, further calculations were made to estimate the stability of oxygen inside the NWs. Fig. 4

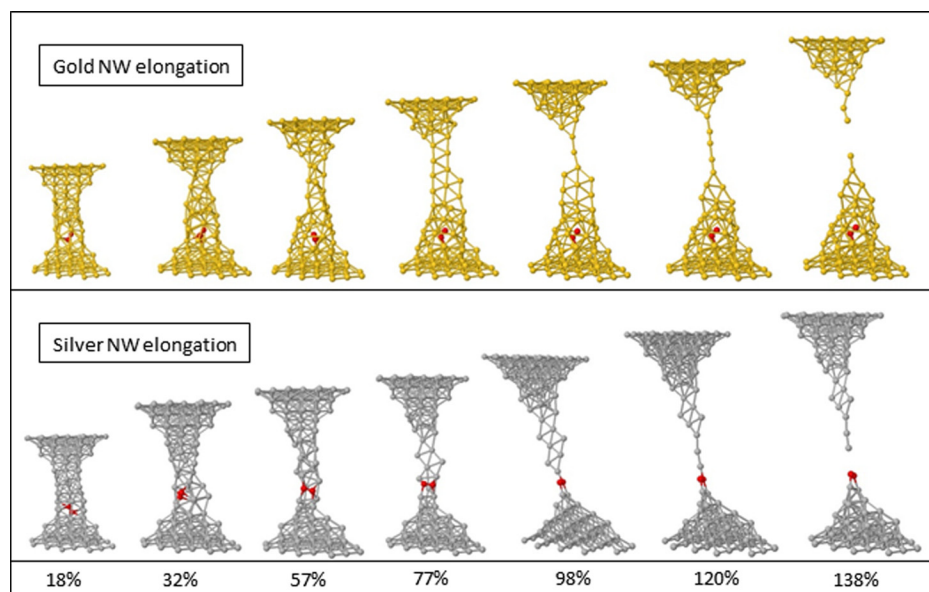


FIG. 2. Atomic configurations of gold and silver NWs obtained after relaxation for representative tensile strains. For both NWs, the O_2 was located initially in the shoulder.

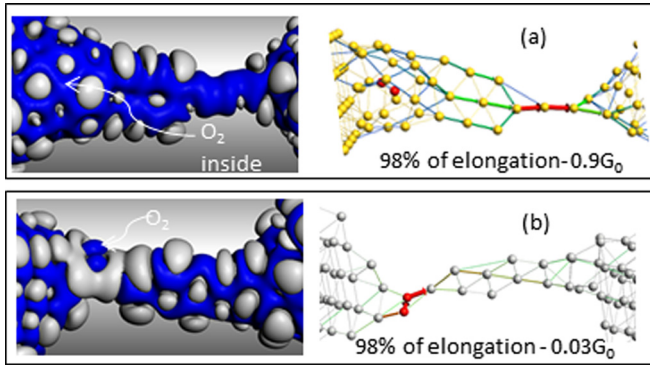


FIG. 3. The iso-surface of the differential electron density (an electron density corresponds to the increase and decrease of the electron density relative to the individual atoms) and the transmission pathways at zero bias at the Fermi level for (a) gold and (b) silver NWs containing an O_2 impurity in the shoulder and elongated 98% from their initial state. The dark (blue) and the light (gray) shades represent an increase and decrease of the differential electron density by $10^{-3} e/\text{\AA}^3$, respectively. The thickness and the colors of the arrows are related to amount of local current between each pair of atoms, and are normalized to the maximum value in each figure.

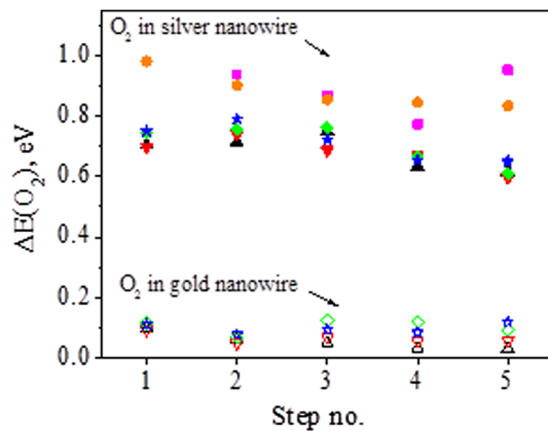


FIG. 4. The increase of the O_2 energy due to interaction with silver (solid symbols) and gold (open symbols) NWs at the initial elongation steps of the studied simulations. The base line energy is given by the isolated and relaxed O_2 .

shows the energy increase of the ($\Delta E(O_2)$) for both NWs calculated at the five initial steps of elongation. This energy increase is related to the interaction with the metallic atoms and was calculated according to Eq. (1). As can be seen in Fig. 4, the oxygen (O_2) inside the silver NWs is less stable

than the oxygen inside the gold NW; in silver, its energy increased by ≈ 0.8 eV, while in gold its energy only increased by ≈ 0.1 eV with respect to the energy of an isolated relaxed oxygen molecule

$$\Delta E(O_2) = E_{O_2}^{\text{non-rlx}} - E_{O_2}^{\text{rlx}}. \quad (1)$$

Here, $E_{O_2}^{\text{non-rlx}}$ is the energy of the two oxygen atoms with the same bond length as inside the NWs and $E_{O_2}^{\text{rlx}}$ is the energy of the isolated oxygen molecule after relaxation.

This energy difference, and therefore, the oxygen stability inside the NW, is related to the differences in O-O bond length inside the metallic NWs. Relatively large bond lengths (1.39 Å to 1.44 Å) were found for the oxygen inside the silver NWs, while smaller bond lengths (1.26 Å to 1.29 Å) were determined for oxygen inside the gold NWs. For the relaxed molecule, the bond length was computed to be 1.23 Å, which is in good agreement with the experimental value of 1.21 Å.⁶⁹ The binding energy of the oxygen inside the metallic NWs was also considered. This energy was computed for the initial steps of the elongation according to Eq. (2). It was found that the oxygen inside the silver is more strongly coupled to the NWs, and its binding energy is ≈ 1.2 eV higher than the binding energy inside the gold NWs

$$E^b(O_2) = E_{\text{NW}+O_2}^{\text{rlx}} - (E_{\text{NW}}^{\text{non-rlx}} + E_{O_2}^{\text{non-rlx}}). \quad (2)$$

Here, $E^b(O_2)$ is the binding energy of the oxygen inside the metallic NWs, $E_{\text{NW}+O_2}^{\text{rlx}}$ is the energy of the relaxed NW with oxygen, after a specific elongation step, $E_{O_2}^{\text{non-rlx}}$ is the energy of the oxygen after removing the metallic atoms, and $E_{\text{NW}}^{\text{non-rlx}}$ is the energy of the metallic NW atoms of the relaxed contaminated NWs but after removing the oxygen atoms.

The DOS of the contaminated gold and silver NWs are quite similar. For both kinds of NWs, the $2p$ electrons of the oxygen mainly interact with the d electrons of the metallic atoms near it. This interaction changes the DOS of the d electrons, and new bands adjacent to the Fermi energy and at ≈ 7 eV appear beneath it. Fig. 5 displays representative DOS of oxygen inside the NW and metallic atoms which are near the oxygen and far from it. The main difference between the Au and the Ag cases is related to the charge transfer between the metallic atom and the O_2 . Mulliken population analysis indicates that the charge transfer to the oxygen molecule in the Ag NW is more than three times higher than the charge transfer to the oxygen molecule in the Au NW. It was found

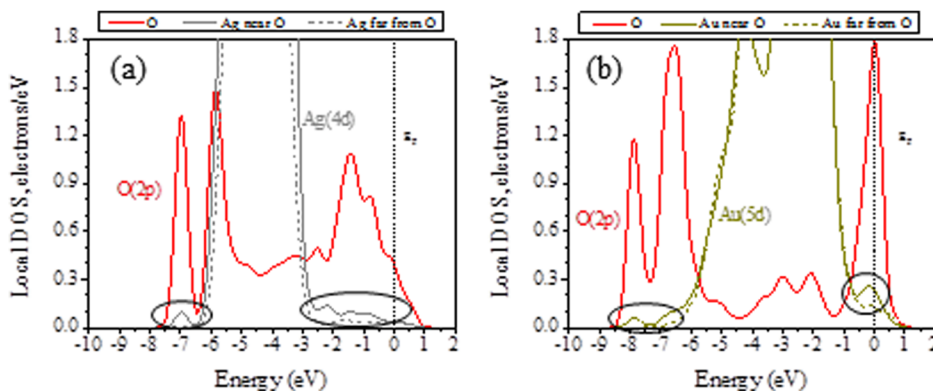


FIG. 5. Representative DOS of atomic oxygen, a metallic atom close to the oxygen, and a metallic atom far from it for the silver NW (a) and the gold NW (b).

that ≈ 0.7 electrons, mostly from the nearest Ag atoms, were transferred to the $2p$ states of the O_2 .

IV. SUMMARY AND CONCLUSIONS

Tensile simulations of pure and oxygen contaminated NWs were performed to study the effect of an internal O_2 impurity on the structure and conductance evolution of gold and silver NWs during elongation. As a comparison, similar simulations were run for the pure NWs as well. At the late elongation steps, the pure NW structures transform to a SAC and the conductance of both converges to $\approx 1 G_0$. However, as was observed in conductance measurements,^{14,15} the contaminated NWs behave differently. At the late steps of the elongation, the presence of oxygen hardly affects the conductance of the gold NWs, but significantly decreases it for the silver NWs.

For both NWs, the electronic characterization shows that the $2p$ electrons of the oxygen interact mainly with the d electrons of the metallic atoms adjacent to the oxygen. However, for the silver NWs, this interaction evolves a higher charge transfer from the NW to the oxygen and therefore it may have greater impact on the conductance. Moreover, for the gold NWs, it was found that the presence of oxygen reinforces the Au-Au binding of the NW adjacent to the oxygen, and therefore, during the elongation, in all of the simulations, the oxygen stays inside the gold NWs, surrounded by gold atoms. In these simulations, the thinning area of the NW down to SAC occurs far from the O_2 . Therefore, the electron depletion of the Au atoms around the oxygen does not affect the conductance at the late steps of the elongation. For the silver NWs, it was found that the presence of oxygen weakens the silver NW in its vicinity. For five out of six different tensile simulations, the Ag-Ag bonds adjacent to the oxygen were broken. In most of these cases, the NW thinning and phase transformations occurred in the vicinity of the oxygen. In addition, the strong binding energy calculated for the internal O_2 with the silver atoms helps the oxygen to be attached to the Ag atoms and to incorporate into the main transmission pathway. At this location, the electron density decrease due to the Ag- O_2 interaction reduces the availability of electrons needed for the conductance.

This study suggests that the different behavior between gold and silver NWs can be related to differences in the charge transfer from the metallic atoms of the NW to the oxygen molecule, and to the ability of the oxygen to incorporate near the main conductance channel at the late steps of the elongation. When the oxygen stays inside the NW (as was the case for the Au NW) it is not affect the conductance, but when it pops out and reaches the thin part on the NW, the charge transfer becomes crucial and decreases the conductance.

¹K. Yanson, O. I. Shklyarevskii, Sz. Csonka, H. van Kempen, S. Speller, A. I. Yanson, and J. M. van Ruitenbeek, *Phys. Rev. Lett.* **95**, 256806 (2005).

²M. Kiguchi, T. Konishi, and K. Murakoshi, *Phys. Rev. B* **73**, 125406 (2006).

³M. Kiguchi, T. Konishi, K. Tasegawa, S. Shidara, and K. Murakoshi, *Phys. Rev. B* **77**, 245421(2008).

⁴M. Kiguchi, D. Djukic, and J. M. van Ruitenbeek, *Nanotechnology* **18**, 035205 (2007).

⁵R. Suzuki, M. Tsutsui, D. Miura, S. Kurokawa, and A. Sakai, *Jpn. J. Appl. Phys., Part 1* **46**, 3694 (2007).

⁶T. Kizuka, *Phys. Rev. B* **77**, 155401 (2008).

⁷Y. Oshima, Y. Kurui, and K. Takayanagi, *J. Phys. Soc. Jpn.* **79**, 054702 (2010).

⁸E. Scheer *et al.*, *Nature* **394**, 154 (1998).

⁹Y. Kurui, Y. Oshima, M. Okamoto, and K. Takayanagi, *Phys. Rev. B* **79**, 165414 (2009).

¹⁰R. H. M. Smit, C. Untiedt, G. Rubio-Bollinger, R. C. Segers, and J. M. van Ruitenbeek, *Phys. Rev. Lett.* **91**, 076805 (2003).

¹¹M. Dreher, F. Pauly, J. Heurich, J. C. Cuevas, E. Scheer, and P. Nielaba, *Phys. Rev. B* **72**, 75435 (2005).

¹²H. Ohnishi, Y. Kondo, and K. Takayanagi, *Nature* **395**, 780 (1998).

¹³D. T. Smith, J. R. Pratt, F. Tavazza, L. E. Levine, and A. M. Chaka, *J. Appl. Phys.* **107**, 084307 (2010).

¹⁴W. H. A. Thijssen, D. Marjenburgh, R. H. Bremmer, and J. M. van Ruitenbeek, *Phys. Rev. Lett.* **96**, 026806 (2006).

¹⁵W. H. A. Thijssen, M. Strange, J. M. J. aan de Brugh, and J. M. van Ruitenbeek, *New J. Phys.* **10**, 33005 (2008).

¹⁶F. Tavazza, L. E. Levine, and A. M. Chaka, *J. Appl. Phys.* **106**, 43522 (2009).

¹⁷N. Agrait, A. L. Yeyati, and J. M. van Ruitenbeek, *Phys. Rep.* **377**, 81 (2003).

¹⁸N. Agrait, G. Rubio, and S. Vieira, *Phys. Rev. Lett.* **74**, 3995 (1995).

¹⁹G. Rubio-Bollinger, P. Joyez, and N. Agrait, *Phys. Rev. Lett.* **93**, 116803 (2004).

²⁰A. Nitzan and M. A. Ratner, *Science* **300**, 1384 (2003).

²¹Z. Qian, R. Li, S. Hou, Z. Xue, and S. Sanvito, *J. Chem. Phys.* **127**, 194710 (2007).

²²M. Brandbyge, J. L. Mozoz, P. Ordejon, J. Taylor, and K. Stokbro, *Phys. Rev. B* **65**, 165401 (2002).

²³Y. Fujimoto and K. Hirose, *Phys. Rev. B* **67**, 195315 (2003).

²⁴Y. J. Lee *et al.*, *Phys. Rev. B* **69**, 125409 (2004).

²⁵M. Zhuang and M. Ernzerhof, *J. Chem. Phys.* **120**, 4921 (2004).

²⁶A. Grigoriev *et al.*, *Phys. Rev. Lett.* **97**, 236807 (2006).

²⁷L. Ke *et al.*, *Nanotechnology* **18**, 095709 (2007).

²⁸S. Barzilai, F. Tavazza, and L. E. Levine, *J. Mater. Sci.* **48**, 6619 (2013).

²⁹F. Tavazza, L. E. Levine, and A. M. Chaka, *Phys. Rev. B* **81**, 235424 (2010).

³⁰F. Tavazza, D. T. Smith, L. E. Levine, J. R. Pratt, and A. M. Chaka, *Phys. Rev. Lett.* **107**, 126802 (2011).

³¹D. Szczesniak and A. Khater, *Eur. Phys. J. B* **85**, 174 (2012).

³²T. Kwapinski, *J. Phys. Condens. Matter* **22**, 295303 (2010).

³³T. Shiota, A. I. Mares, A. M. C. Valkering, T. H. Oosterkamp, and J. M. van Ruitenbeek, *Phys. Rev. B* **77**, 125411 (2008).

³⁴G. Robio-Bollinger, C. de las Heras, E. Bascones, N. Agrait, F. Guinea, and S. Vieira, *Phys. Rev. B* **67**, 121407 (2003).

³⁵E. Anglada, J. A. Torres, F. Yndurain, and J. M. Soler, *Phys. Rev. Lett.* **98**, 096102 (2007).

³⁶F. Tavazza, L. E. Levine, and A. M. Chaka, *Comput. Theor. Chem.* **987**, 84 (2012).

³⁷S. R. Bahn, N. Lopez, J. K. Norskov, and K. W. Jacobsen, *Phys. Rev. B* **66**, 081405R (2002).

³⁸F. D. Novaes, A. J. R. da Silva, E. Z. da Silva, and A. Fazzio, *Phys. Rev. Lett.* **96**, 016104 (2006).

³⁹E. Z. da Silva, F. D. Novaes, A. J. R. da Silva, and A. Fazzio, *Nanoscale Res. Lett.* **1**, 91 (2006).

⁴⁰N. V. Skorodumova and S. I. Simak, *Phys. Rev. B* **67**, 121404R (2003).

⁴¹N. V. Skorodumova, S. I. Simak, A. E. Kochetov, and B. Johansson, *Phys. Rev. B* **75**, 235440 (2007).

⁴²S. B. Legoas, V. Rodrigues, D. Ugarte, and D. S. Galvao, *Phys. Rev. Lett.* **93**, 216103 (2004).

⁴³P. Velez, S. A. Dassie, and E. P. M. Leiva, *Phys. Rev. B* **81**, 125440 (2010).

⁴⁴E. Hobi, Jr., A. Fazzio, and A. J. R. da Silva, *Phys. Rev. Lett.* **100**, 056104 (2008).

⁴⁵A. E. Kochetov and A. S. Mikhaylushkin, *Eur. Phys. J. B* **61**, 441 (2008).

⁴⁶C. Zhang, R. N. Barnett, and U. Landman, *Phys. Rev. Lett.* **100**, 046801 (2008).

⁴⁷R. N. Barnett, H. Hkkinen, A. G. Scherbakov, and U. Landman, *Nano Lett.* **4**, 1845 (2004).

- ⁴⁸H. Ishida, *Phys. Rev. B* **75**, 205419 (2007).
- ⁴⁹H. Ishida, *Phys. Rev. B* **77**, 155415 (2008).
- ⁵⁰P. Jelínek, R. Prez, J. Ortega, and F. Flores, *Phys. Rev. B* **77**, 115447 (2008).
- ⁵¹D. Cakir and O. Gulseren, *Phys. Rev. B* **84**, 85450 (2011).
- ⁵²Y. Qi, D. Guan, Y. Jiang, Y. Zheng, and C. Liu, *Phys. Rev. Lett.* **97**, 256101 (2006).
- ⁵³M. Strange, K. S. Thygesen, J. P. Sethna, and K. W. Jacobsen, *Phys. Rev. Lett.* **101**, 096804 (2008).
- ⁵⁴Commercial software is identified to specify procedures. Such identification does not imply recommendation by the National Institute of Standards and Technology.
- ⁵⁵B. Delley, *J. Chem. Phys.* **92**, 508 (1990).
- ⁵⁶B. Delley, *J. Chem. Phys.* **113**, 7756 (2000).
- ⁵⁷J. P. Perdew, S. Burke, and M. Ernzerhof, *Phys. Rev. Lett.* **77**, 3865 (1996).
- ⁵⁸B. Delley, *Phys. Rev. B* **66**, 155125 (2002).
- ⁵⁹P. Pulay and G. Fogarasi, *J. Chem. Phys.* **96**, 2856 (1992).
- ⁶⁰J. Baker, A. Kessi, and B. Delley, *J. Chem. Phys.* **105**, 192 (1996).
- ⁶¹H. J. Monkhorst and D. Pack, *J. Phys. Rev. B* **13**, 5188 (1976).
- ⁶²G. D. Mahan, *Comments Condens. Matter Phys.* **16**, 333 (1994).
- ⁶³S. Datta, *Electron Transport in Mesoscopic Systems* (Cambridge University Press, Cambridge, England, 1995).
- ⁶⁴Atomistix ToolKit version 11.08, QuantumWise A/S.
- ⁶⁵J. Taylor, H. Guo, and J. Wang, *Phys. Rev. B* **63**, 245407 (2001).
- ⁶⁶K. Stokbro *et al.*, *Phys. Rev. B* **82**, 075420 (2010).
- ⁶⁷J. Cerda and F. Soria, *Phys. Rev. B* **61**, 7965 (2000).
- ⁶⁸J. H. Ammeter, H. B. Burgi, J. C. Thibault, and R. Hoffmann, *J. Am. Chem. Soc.* **100**, 3686 (1978).
- ⁶⁹R. Weast, *CRC Handbook of Chemistry and Physics* (CRC Press, Inc., Boca Raton, FL, 1985).